

# **Supporting Information**

## **Unidirectional mechanistic valved mechanisms for ammonia transport in GatCAB**

Jiyoung Kang<sup>1</sup>, Shigehide Kuroyanagi<sup>1</sup>, Tomohiro Akisada<sup>2</sup>, Yohsuke Hagiwara<sup>1</sup>, and  
Masaru Tateno<sup>2\*</sup>

<sup>1</sup> Graduate School of Pure and Applied Sciences, University of Tsukuba, Tennodai  
1-1-1, Tsukuba Science City, Ibaraki 305-8571, Japan.

<sup>2</sup> Graduate School of Life Science, University of Hyogo, 3-2-1 Kouto, Kamigori-cho,  
Ako-gun, Hyogo 678-1297, Japan.

\*To whom correspondence should be addressed.

E-mail: tateno@sci.u-hyogo.ac.jp

## **Contents**

- S1. Evaluation of interaction energies of ammonia and aspartate**
- S2. Summary of all MD simulations**
- S3. Crystal water molecules observed in the channels**
- S4. Evaluation of the force constant used in umbrella sampling**
- S5. Structural stability of GatCAB in MD simulations**
- S6. Free energy profile for backward flow: another PMF calculation**
- S7. References**

### S1. Evaluation of interaction energies of ammonia and protein

The interaction energies between ammonia (the RESP charges; see 2.1 in text) and the protein (ff99sb) were verified by comparison with the values obtained by *ab initio* calculations, since these interactions are substantial in this study. As shown in Table S1, we found that both values are close, whereas the value calculated using gaff (generalized amber force field) is not consistent with the other values.

Table S1. A typical example of the comparison of interaction energies. Interaction energies between NH<sub>3</sub> and an aspartate (Asp) side chain, calculated using various methodologies, are shown. The structural model shown in Fig. S1 was utilized for the calculations.

	<i>ab initio</i> calculation	RESP <sup>1</sup>	gaff <sup>2</sup>
Interaction Energy [kcal/mol]	-13.3	-11.2	-5.7

<sup>1</sup> See the text (section 2.1).

<sup>2</sup> The generalized amber force field (gaff) was employed for the atomic charges of NH<sub>3</sub>.

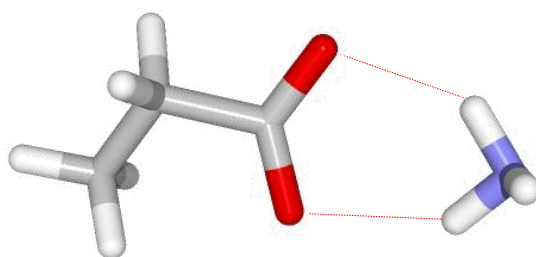


Figure S1. Calculation model of NH<sub>3</sub> and Asp.

## S2. Summary of all MD simulations

Table S2. Protocols of MD simulations of GatCAB including NH<sub>3</sub>.

	SMD1	SMD2	SMD3	SMD4	SMD5	SMD6
form of ammonia						
molecule			NH <sub>3</sub>			
initial position of ammonia	IP1 <sup>1</sup>	IP1 <sup>1</sup>	IP2 <sup>2</sup>	IP2 <sup>2</sup>	IP3 <sup>3</sup>	IP3 <sup>3</sup>
crystallographic waters	○	×	○	×	○	×

<sup>1</sup> NH<sub>3</sub> was placed at the position occupied by the crystallographic water that hydrogen-bonds to the substrate (Gln) bound in the glutaminase site.

<sup>2</sup> NH<sub>3</sub> was placed at the position of the crystallographic water that hydrogen-bonds to Arg200 in GatA.

<sup>3</sup> NH<sub>3</sub> was placed at the position of the crystallographic water that hydrogen-bonds to Asn81 in GatA.

Table S3. Protocols of MD simulations of GatCAB including  $\text{NH}_4^+$ .

	SMD7	SMD8	SMD9	SMD10	SMD11	SMD12
form of ammonia						
molecule			$\text{NH}_4^+$			
initial position of ammonia	IP1 <sup>1</sup>	IP1 <sup>1</sup>	IP2 <sup>2</sup>	IP2 <sup>2</sup>	IP3 <sup>3</sup>	IP3 <sup>3</sup>
crystallographic waters	○	×	○	×	○	×

Table S4. Protocols of PMF calculations.

	TMD1	TMD2	TMD3	TMD4	TMD5
form of ammonia					
molecule	$\text{NH}_3$	$\text{NH}_4^+$	$\text{NH}_3$	$\text{NH}_4^+$	$\text{NH}_3$
initial position of ammonia	IP4 <sup>4</sup>	IP4 <sup>4</sup>	IP4 <sup>4</sup>	IP4 <sup>4</sup>	IP5 <sup>5</sup>
Channel	Gate 1	Gate 1	Gate 2	Gate 2	Gate 2

<sup>4</sup>  $\text{NH}_3$  or  $\text{NH}_4^+$  was placed inside the glutaminase site.

<sup>5</sup>  $\text{NH}_3$  was placed inside Channel 2.

### S3. Crystal water molecules observed in the channels

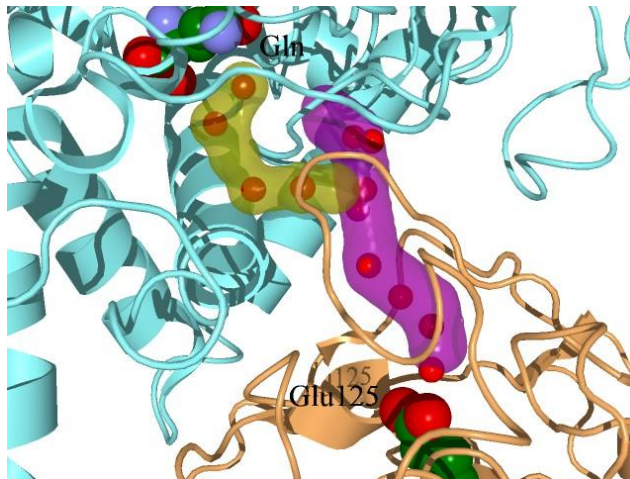


Figure S2. Crystal water molecules observed in the channels. Channels 1 and 2 are colored yellow and magenta, respectively. The oxygen atoms of the water molecules are depicted by red spheres.

#### S4. Evaluation of the force constant used in umbrella sampling.

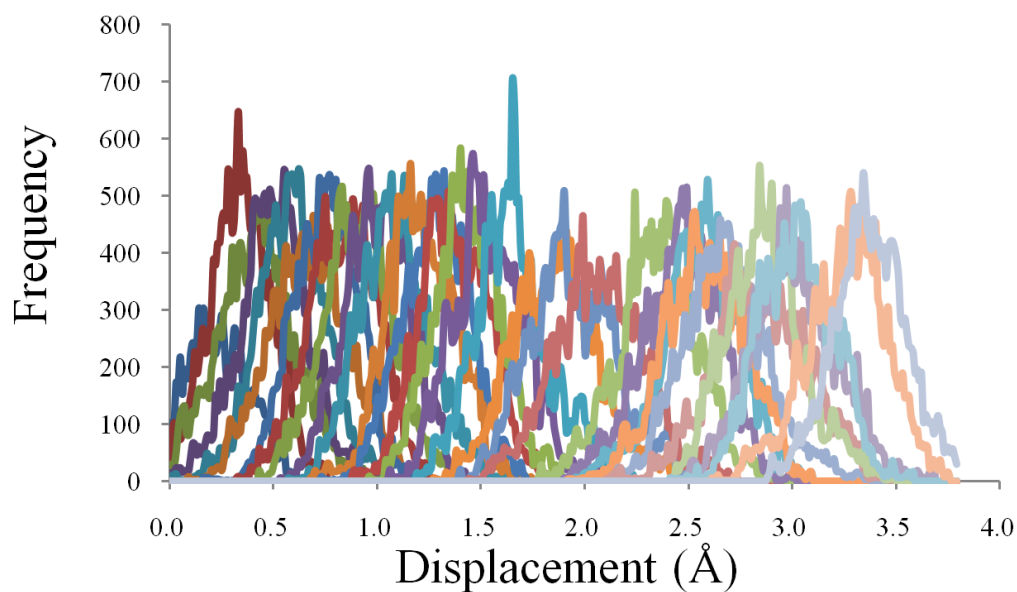


Figure S3. The histogram of the reaction coordinate (displacement of  $\text{NH}_3$ ) obtained in the PMF calculation with respect to the  $\text{NH}_3$  passage through Gate 2.

#### S5. Structural stability of GatCAB in MD simulations

The results of SMD1-12 and the multiple MD simulations are shown in Figs. S4 and S5, respectively. As for the latter, the results of the calculations starting from various snapshots of SMD7 are shown as a typical example, among the calculations starting from the snapshots of SMD1-12.

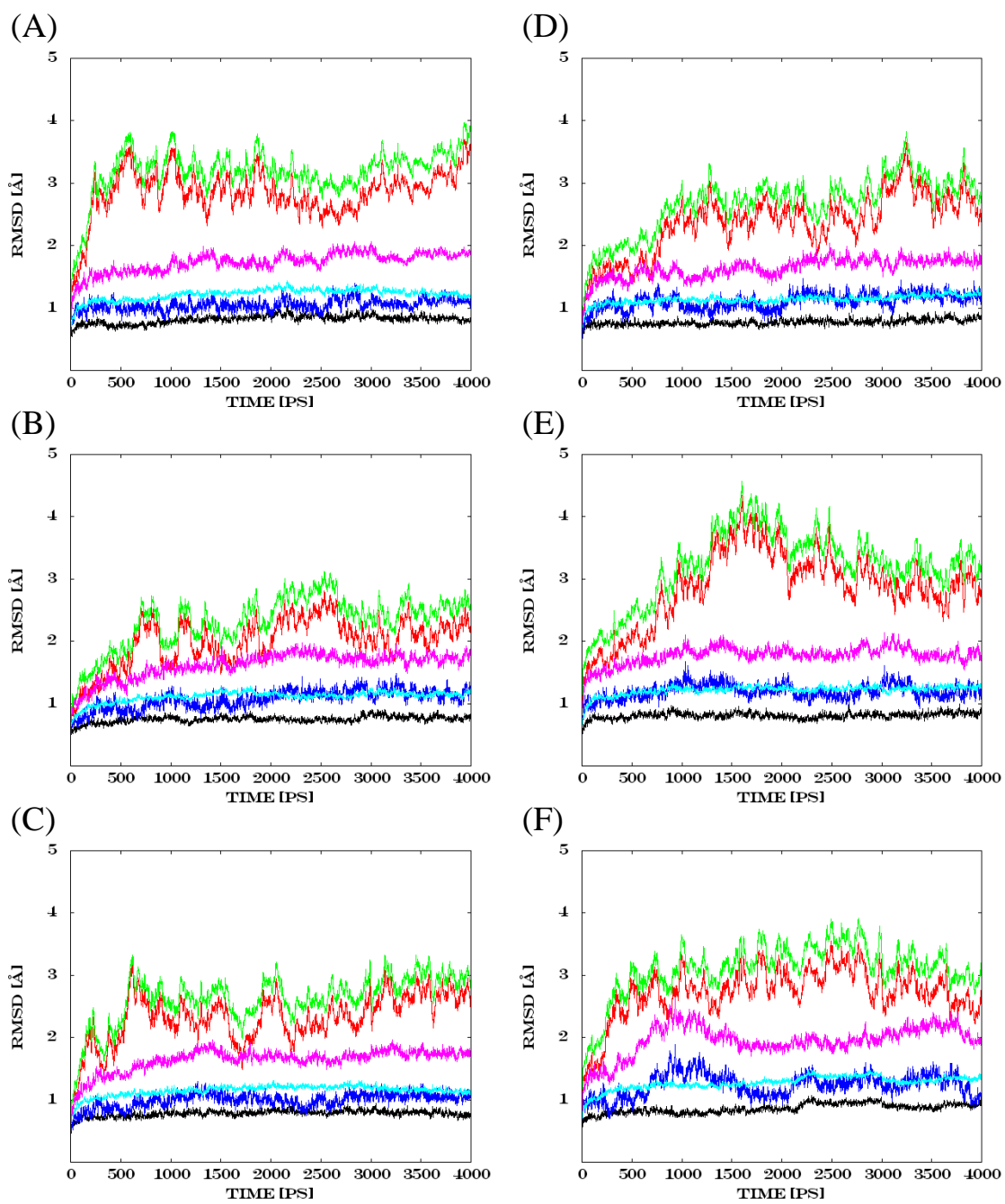


Figure S4 (continued)



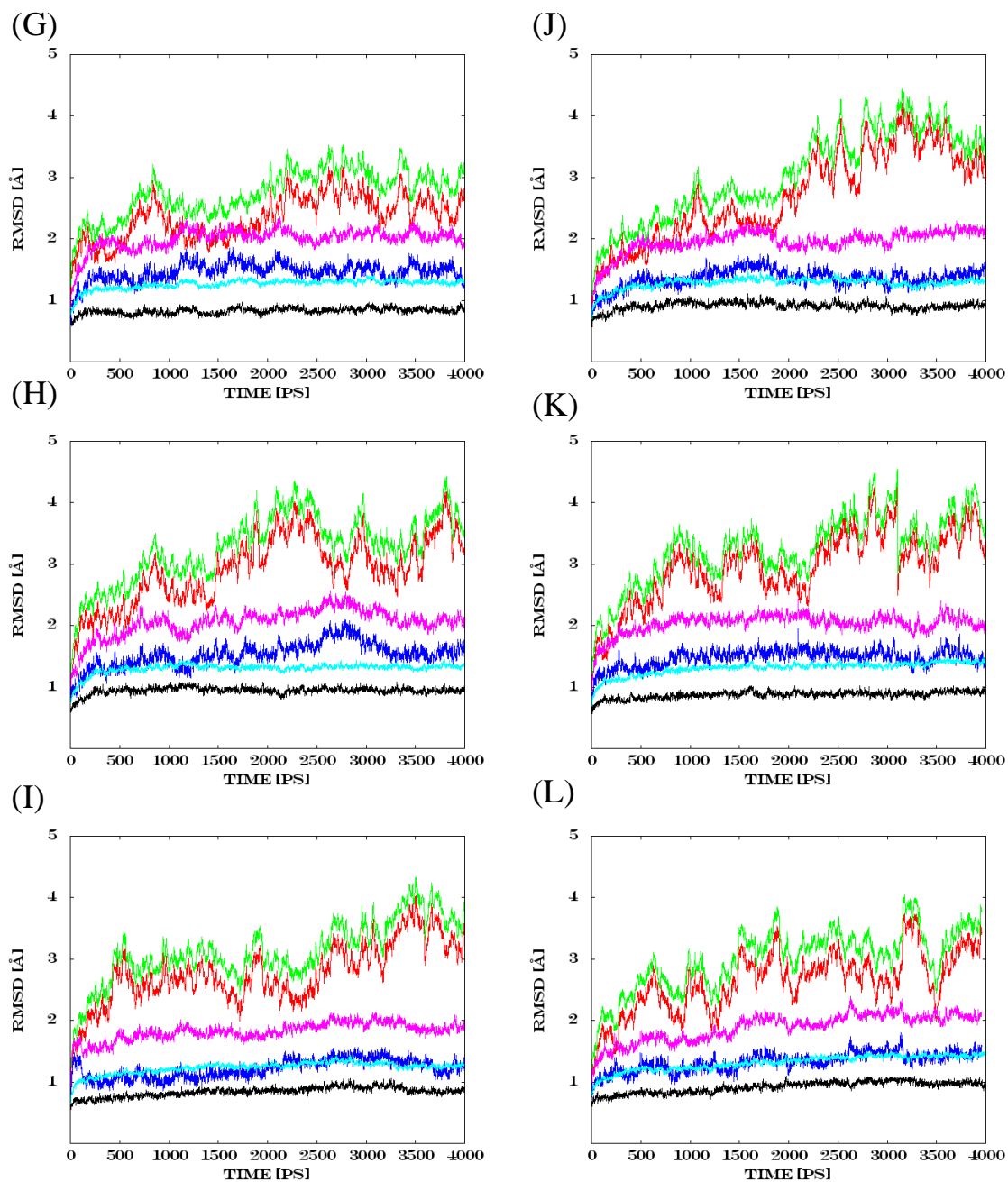
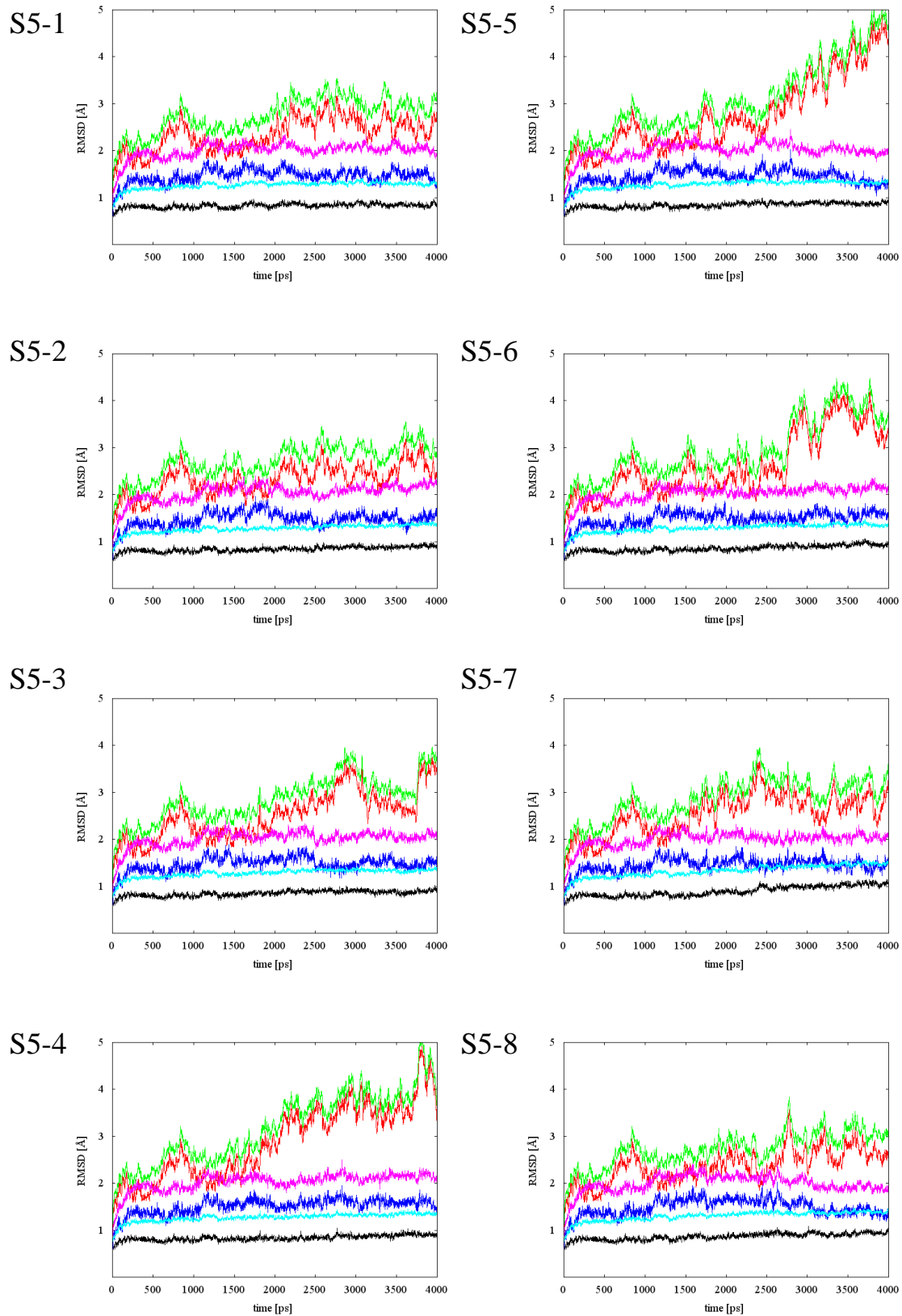
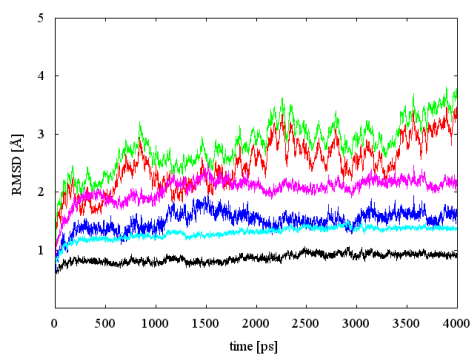


Figure S4. Trajectories of the RMSDs of the three subunits of GatCAB (with respect to the C $\alpha$ /heavy atoms), i.e., GatA (black/cyan), GatB (red/green), and GatC (blue/magenta). SMD1-12 are shown in (A)-(L), respectively.

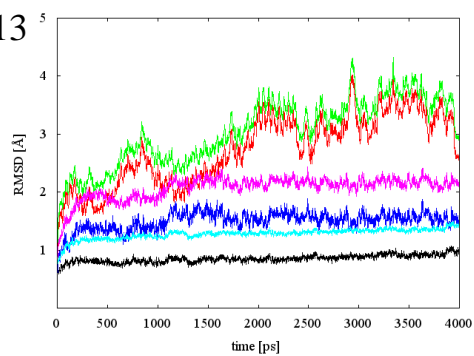
Typical results of the multiple MD simulations are shown in Fig. S5.



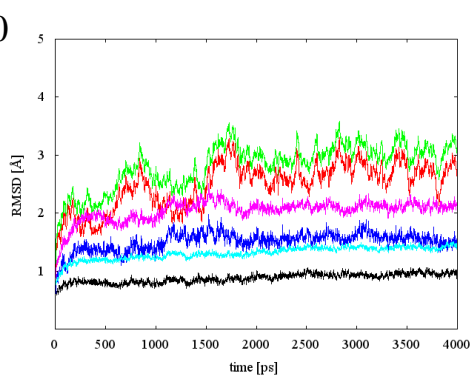
S5-9



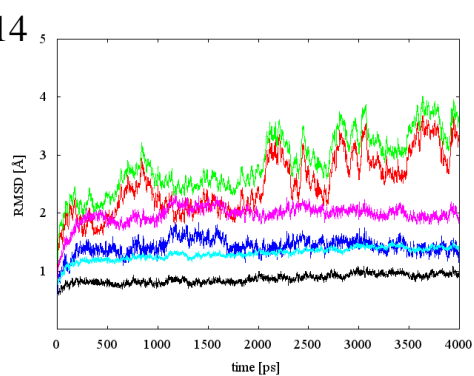
S5-13



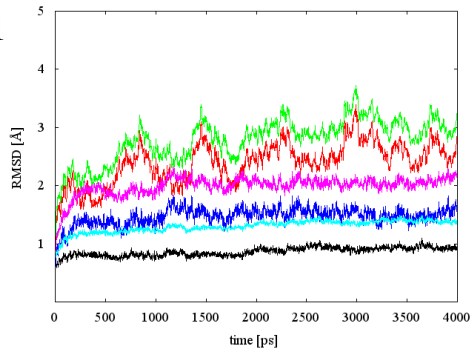
S5-10



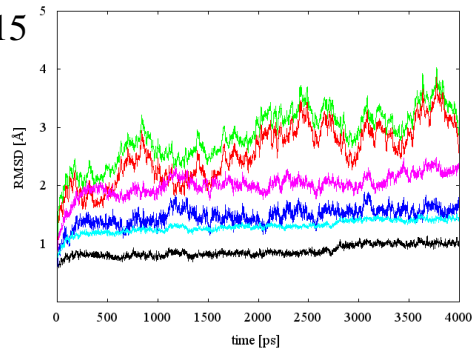
S5-14



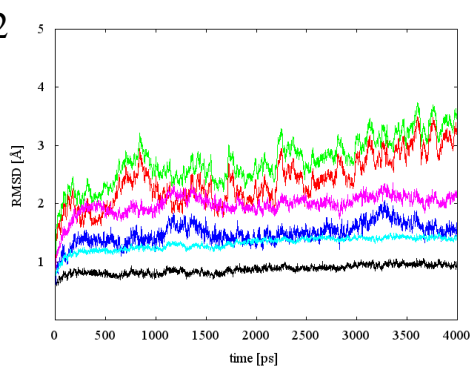
S5-11



S5-15



S5-12



S5-16

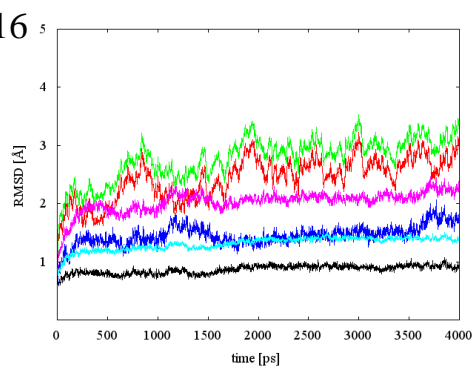
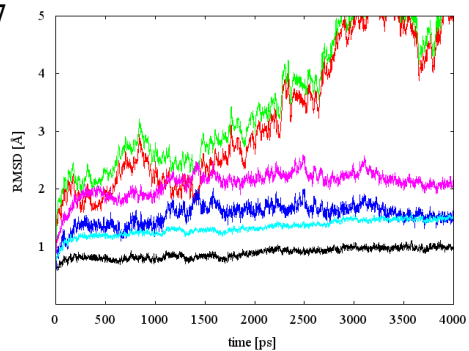
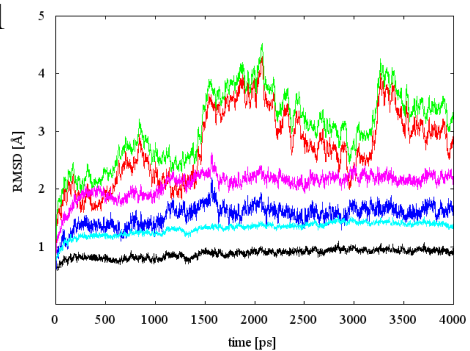


Figure S5 (continued)

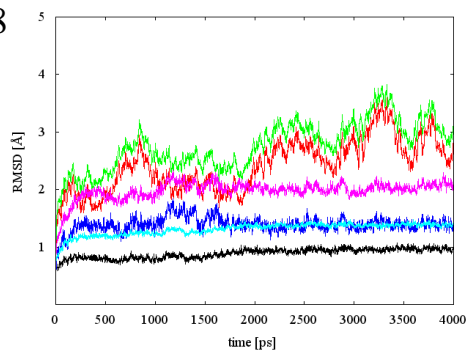
S5-17



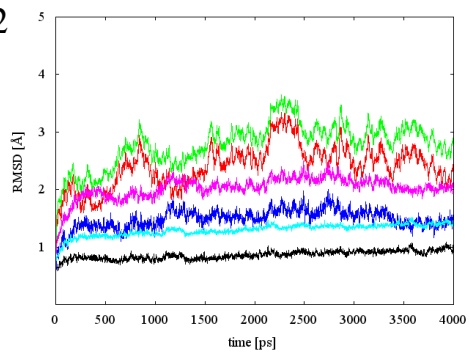
S5-21



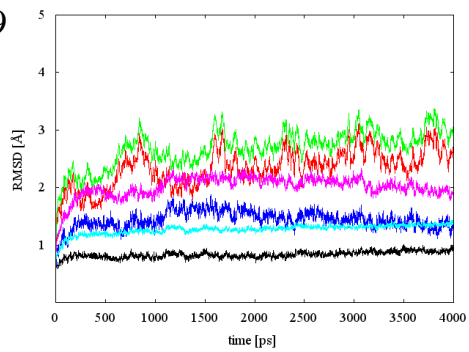
S5-18



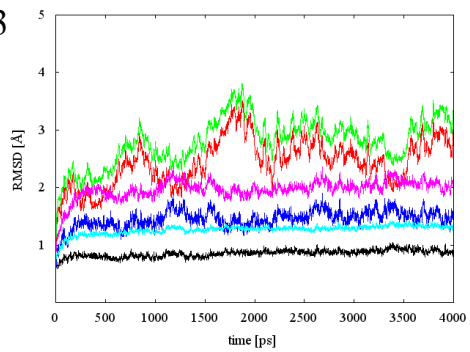
S5-22



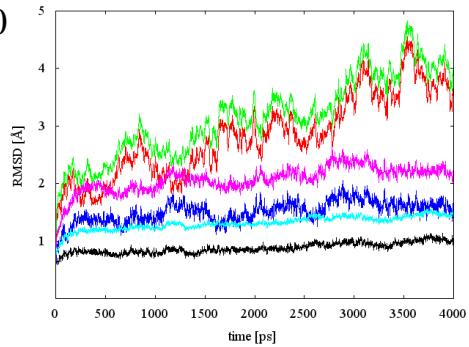
S5-19



S5-23



S5-20



S5-24

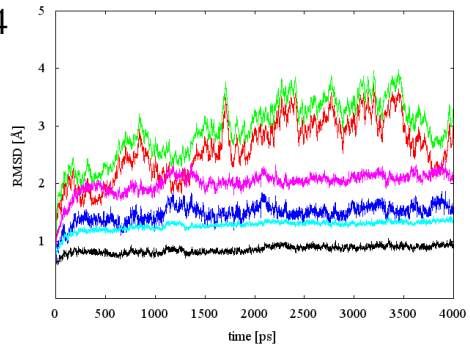


Figure S5 (continued)

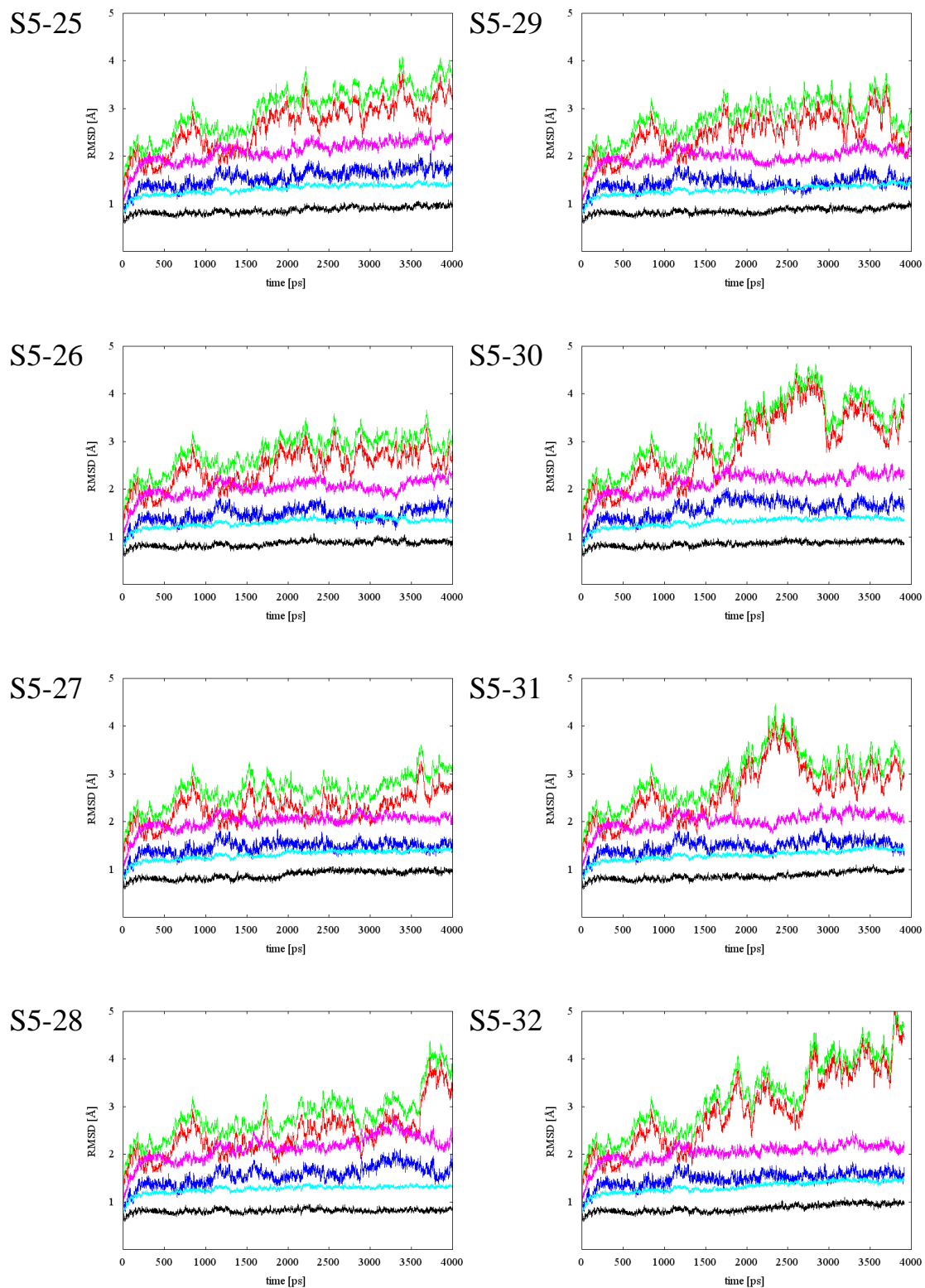


Figure S5. A typical example of a set of 32 trajectories of the RMSDs obtained by the

multiple MD simulations, which started from various snapshots of SMD7. The color index is the same as that used in Fig. S4.

### **S6. Free energy profile for backward flow: another PMF calculation**

As discussed in the text, the PMF calculation (TMD5) to evaluate the backward transport of ammonia molecules through Gate 2 failed (see text; section 3.4). This might have been a consequence of the inappropriate reaction coordinate (the displacement of an ammonia molecule). Therefore, to further validate the mechanisms of the unidirectional transport, we evaluated the free energy by employing the  $\chi_1$  angle of Phe206 as the reaction coordinate. In fact, this angle transited from 160 to 60 degrees, when the forward transport of ammonia molecules occurred (see text; Fig. 7A). Accordingly, it can be assumed that the backward transport should also be driven by the rotation of this angle.

To validate this hypothesis, we performed a PMF calculation starting from a snapshot of SMD6, where the  $\chi_1$  angle of Phe206 was 160 degrees. For each window, a 100 ps MD simulation was performed with a harmonic constraint, in which the equilibrated position was sequentially varied from 160 to 300 degrees (for the backward transport) and 160 to 110 degrees (for the forward transport), with a 5 degree step for each window. The force constant was set to  $1,000 \text{ kcal mol}^{-1} \text{ rad}^{-2}$ . The free energy profile was calculated by using WHAM<sup>1-2</sup> (Fig. S4).

These PMF calculations finished normally (Fig. S4). For the backward transport, the activation barrier was estimated to be as large as  $\sim 100 \text{ kcal/mol}$ . Therefore, the rotation

of the  $\chi_1$  angle of Phe206 for the backward transport (i.e., from 160 to 300 degrees) is unlikely to occur. On the other hand, the activation barrier for the forward transport (i.e., from 160 to 110 degrees) was estimated to be small ( $\sim 3$  kcal/mol). This is due to the mechanical stopper formed by the Ala207 backbone (HN-). Thus, we concluded that the unidirectional transport through Gate 2 is feasible.

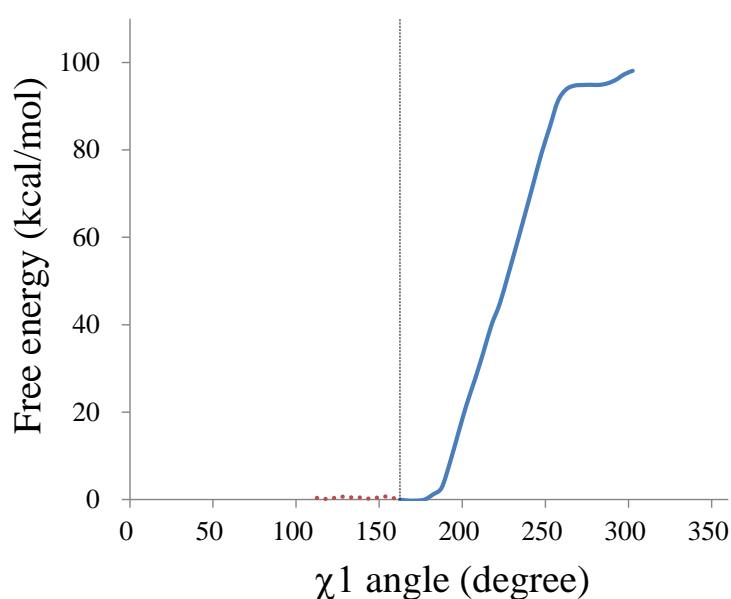


Figure S6. Free energy profile obtained by performing PMF calculations with respect to the  $\chi_1$  angle of Phe206. The blue line and the red dotted line show the results for the backward (160 to 300 degrees) and forward transport (160 to 110 degrees), respectively.

## S7. References

- (1) Kumar, S.; Rosenberg, J. M.; Bouzida, D.; Swendsen, R. H.; Kollman, P. A., *Journal of Computational Chemistry* **1995**, *16*, 1339-1350.
- (2) Kumar, S.; Rosenberg, J. M.; Bouzida, D.; Swendsen, R. H.; Kollman, P. A., *Journal of Computational Chemistry* **1992**, *13*, 1011-1021.